Approaches to structure and dynamics of biological systems by electron-paramagnetic-resonance spectroscopy

Scarpelli, F.

Chapter 1. Introduction

The study of the structure and dynamics of proteins and enzymes is crucial in the understanding of the function of such biological systems. Structure first refers to the geometrical structure, as a result of backbone folding and local arrangement of amino-acid side chains. Secondly, structure refers to electron structure, in particular at the active sites of proteins and enzymes where the transformations take place. Dynamics refers to structural changes as a response to changes in the environment of the system and to relative rearrangement of different parts of its molecules, for example during complex formation and substrate binding.
Electron paramagnetic resonance (EPR), the technique central to all the experiments reported in this thesis, is well suited to study protein structure and dynamics. By its nature, the EPR signal represents the fingerprint of the electronic wave function of a paramagnetic site. Moreover, the interactions of the electron spin with nearby nuclear spins may show up and provide information about the delocalized nature of the electronic wave function. In case more electron spins are present, their dipolar interaction contains information about the distance and the mutual orientation of the electron spins. In order to obtain this structural and dynamic knowledge from EPR experiments, both continuous-wave (cw) and pulsed microwave excitation have been applied, and samples as diverse as single crystals, solution and membranes were studied.
The EPR spectroscopy detects unpaired electrons. In proteins, these may be present naturally as radicals or paramagnetic transition metal ions. Proteins that do not have unpaired electrons can also be studied, but they require extrinsic paramagnetic probes called spin labels. Spin labels are nitroxide derivatives with a stable unpaired electron and a functional group that allows its site-specific attachment to a protein. The most popular amino-acid residues used to attach spin labels are cysteine residues, which, if necessary, can be introduced into the protein structure using molecular biology techniques. In the research described in this thesis both transition metal ions, such as Cu(II) and Fe(III), and nitroxide spin labels have been used.
The work described in this thesis comprised both methodological developments and the application of EPR to specific research questions.

In the next section, I first briefly describe the basic theory of EPR, and subsequently shortly introduce the research reported in Chapters 2 to 5.

1.1 Background of EPR

In EPR experiments, the electron (and nuclear) spins interact with an external magnetic field (static field, oscillatory radiofrequency or microwave field) and with other spins, i.e., other magnetic dipoles within the sample. The interactions of spins with their environment concern the interactions of magnetic dipoles with each other and with external magnetic fields. In magnetic resonance, the external magnetic field defines a unique direction in the laboratory frame. Generally the interactions of spins are anisotropic and they depend on the orientation of the molecule with respect to the laboratory frame (external magnetic field). The EPR spectra of systems in the solid state, such as crystals (ordered arrays of molecules) and frozen solutions (disordered arrays of molecules), reveal anisotropic interactions

.

1.1.1 Spin Hamiltonian

The interaction between the electron spin (S) and the external magnetic field is called electron Zeeman (H_{EZ}) interaction and the interaction between the electron spin and the nuclear spin (I) is called hyperfine interaction (H_{HF}). The spin Hamiltonian for an S=1/2 system can be written as

$$H = H_{EZ} + H_{HF} = \beta_e \vec{B}_0 \vec{\vec{g}} \vec{S} + \vec{S} \vec{\vec{A}} \vec{I} \quad . \tag{1}$$

Here β_e is the electron Bohr magneton, $\vec{B}_0$ is the external magnetic field, $\vec{\vec{g}}$ is the g-tensor and $\vec{\vec{A}}$ is the hyperfine tensor. The hyperfine term can be written as the sum of the Fermi contact interaction and the dipole-dipole coupling between the electron spin and the nuclear spin [1]. In the following equation, the first term describes the Fermi contact interaction and the second one the dipole-dipole coupling between the electron spin and the nuclear spin.

$$H_{HF} = a_{iso}\vec{S}\vec{I} + \frac{\mu_0}{4\pi} g\beta_e g_n \beta_n \left[\frac{3\left(\vec{S}\vec{r}\right)\left(\vec{I}\vec{r}\right)}{r^5} - \frac{\vec{S}\vec{I}}{r^3} \right] \quad , \qquad (2)$$

where a_{iso} is the isotropic hyperfine constant, μ_0 is the permeability of vacuum, g and g_n are respectively the electron and the nuclear g factors, β_n is the nuclear Bohr magneton and $\vec{r}$ is the vector that joins the electron spin and the nuclear spin and r its magnitude.
If the system has two unpaired electrons, the dipole-dipole coupling between the two electron spins (S_1 and S_2) has to be taken into account. It is similar to the electron-nuclear-dipole interaction in Eq. 2, and for the magnetic field parallel to z-axis can be written as

$$H_{DD} = \frac{\mu_0}{4\pi} \frac{g_1 g_2 \beta_e^2}{r_{12}^3} \left(1 - 3\cos^2\theta\right) \left(S_{1z}S_{2z} - \frac{1}{2}S_{1x}S_{2x} - \frac{1}{2}S_{1y}S_{2y} \right), \qquad (3)$$

where g_1 and g_2 are the g factors of the two electrons, r_{12} is the magnitude of the vector that joins the two electrons and θ is the angle between the static magnetic field and the vector that joins the two electrons (Fig. 1).

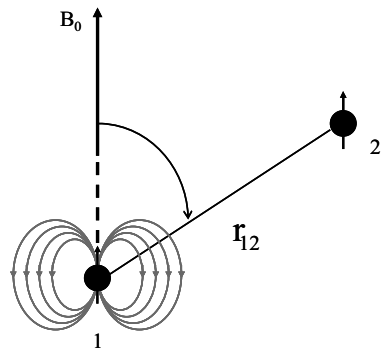

Fig. 1: Schematic representation of the electron-electron dipolar interaction. The two black circles represent the electrons.

1.2 The anisotropy of the g-tensor of a metal center in a protein: single crystal EPR

The Zeeman interaction in Eq. 1 describes the interaction between the spin of an unpaired electron and the external magnetic field. For such an electron in a transition-metal ion, g is anisotropic and is described by the tensor $\vec{\vec{g}}$. The principal axes of g (x, y and z) have a well-defined orientation with respect to the ligands that are bound to the transition-metal ion (Fig. 2). The directions of the principal axes contain information about the electronic structure of the center and they can be determined by single crystal EPR [2].

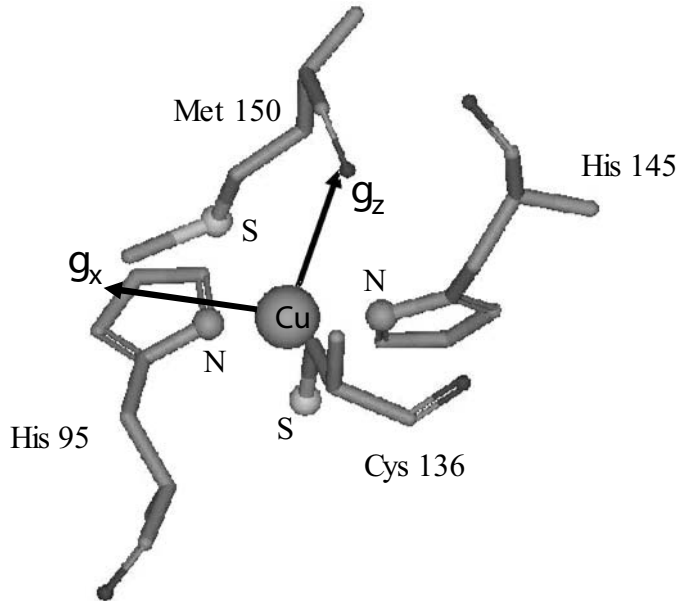

Fig. 2: The directions of the x and z principal axes of the g-tensor of the type-1 copper site of an azurin protein. The histidines (His) and the cysteine (Cys) ligands are approximately in one plane. The g_z axis is approximately perpendicular to the N-Cu-N plane [2].

The Fig. 3a shows the orientation of the magnetic field $\vec{B}_0$ in the g-tensor principal axes system. The field of resonance changes as a function of the orientation of $\vec{B}_0$ and if the field is oriented along one of the principal directions of g the resonance position is characterized by the corresponding g value. This is illustrated in Fig. 3b, where the resonance fields correspond to g_z and g_x for fields parallel to z and x. Measuring the resonance field for a single crystal as a function of the orientation of the magnetic field with respect to the crystal, the full tensor can be obtained.

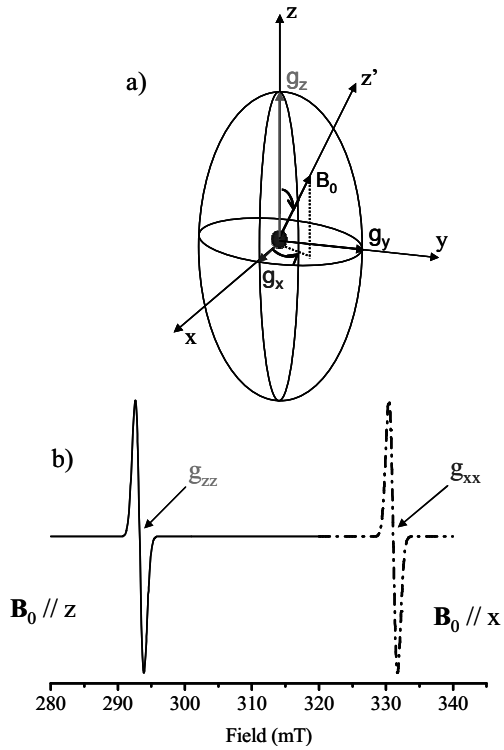

Fig. 3: A paramagnetic center and the principal axes of its g-tensor. (a) The molecular frame (xyz) of the paramagnetic center (dot) is defined by the direction of the principal axes of the g-tensor. Also shown is the direction of the z axis of the laboratory frame (z'). The $\mathbf{B}_0$ is shown parallel to z'. (b) The EPR spectrum for $\mathbf{B}_0$ parallel to z and parallel to x.

The research in Chapter 2 concerns the determination of $\vec{\vec{g}}$ of the type-2 copper site (Cu(II), S=1/2) in the nitrite reductase protein. These experiments have been performed on a single crystal of the protein by EPR at 95 GHz. The analysis is complicated because of the presence of several paramagnetic sites in the crystal, which results in a multitude of overlapping bands [2]. The determination of the directions of the principal axes is described and the results are discussed in terms of the electronic structure of the copper center.

1.3 Averaging of the anisotropic spin interactions: spin-label mobility by EPR

While the anisotropy of the magnetic interaction yields information on the electronic structure, dynamics can be obtained from incomplete averaging of anisotropic interactions. Dynamics in proteins is often studied using spin labels. These are stable nitroxide radicals in which the unpaired electron is delocalized over the nitrogen and the oxygen (Fig. 4).

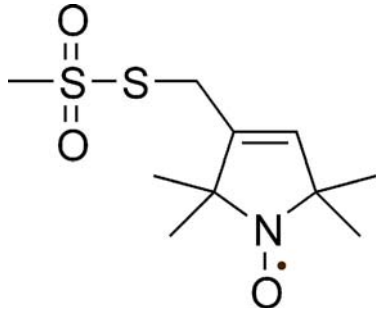

Fig. 4: Chemical structure of a nitroxide spin-label. The black dot represents the unpaired electron.

An isotropic EPR spectrum of such a spin label is shown in Fig. 5a. The three lines of this spectrum result from the hyperfine interaction between the electron spin S = ½ and the nitrogen nuclear spin I = 1. This EPR spectrum one observes for a spin label freely tumbling in solution; the fast rotation of the molecules averages the anisotropy of the interaction

between $\vec{S}$ and $\vec{B}_0$ and between $\vec{S}$ and $\vec{I}$, resulting in an isotropic spectrum. In this case, the separation between the EPR lines is a_{iso}, which comes from the Fermi contact term in the hyperfine Hamiltonian (Eq. 2).

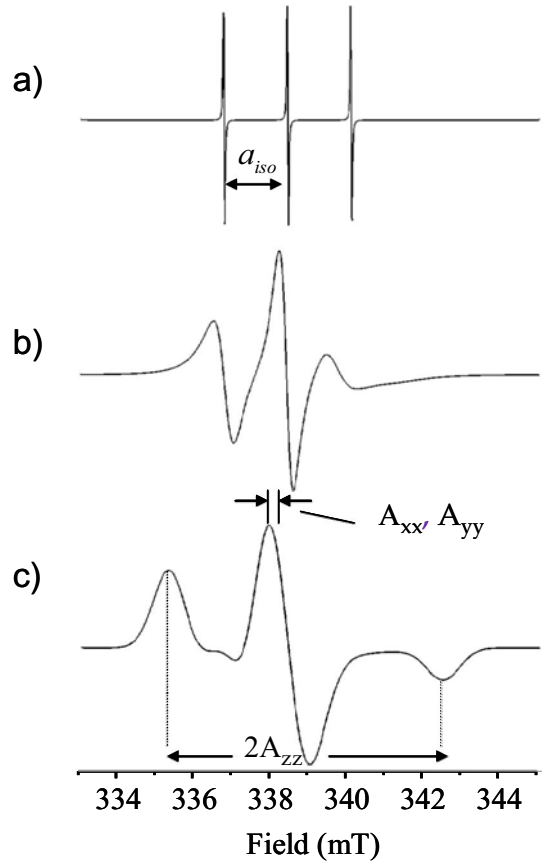

Fig. 5: Effect of the rotational-correlation time (τ_c) on the line shape of EPR spectra of a nitroxide spin-label. (a) The simulated EPR spectrum of a nitroxide spin label with τ_c = 10 ps (liquid solution). (b) The simulated EPR spectrum of a nitroxide spin label with τ_c = 3 ns (intermediate case). (c) The simulated EPR spectrum of an immobilized nitroxide spin label (frozen solution).

In Fig. 5c, the EPR spectrum of a spin label in frozen solution is shown. Here, the molecules are randomly oriented with respect to $\vec{B}_0$ and immobilized. The so-called powder spectrum results from the summation over all the possible orientations. The lines are shifted and broadened relative to the isotropic spectrum because of the anisotropic Zeeman and hyperfine interactions. Fig. 5b illustrates the EPR spectrum of a spin label in an intermediate situation, between the liquid and the frozen state. In this case, the rotation of the molecules is not fast enough to fully average the anisotropy of the spin interactions and the EPR spectrum shows a broadening with respect to the spectrum in Fig. 5a. From the amount of broadening, the rotation-correlation time can be obtained. Therefore, the line shape analysis of such EPR spectra reveals information about the mobility of the spin label and about the local dynamics and possibly local structure elements of the part of the protein to which the spin label is attached [3].
Chapter 3 deals with the mobility of spin labels attached to ten surface positions of a cytochrome c peroxidase in solution. Results are being discussed in the context of the secondary structure of the protein and of the rotation-correlation time of the spin labels.

1.4 Electron dipole-dipole interaction: distance measurements for structure determination

The EPR spectroscopy can be used to measure distances which serve to determine the structure of biological systems. It makes use of the dipolar interaction between spins (Eq. 3 and Fig. 1) to measure distances in the range between 0.8 nm and 10 nm [4] (Fig. 6). Continuous wave (cw) EPR is well suited for the distance range between 0.8 nm and 2.5 nm [4] (Fig. 6). Larger distances, up to 10 nm (Fig. 6), have been measured by pulse techniques, which separate the dipole-dipole interaction of the electron spins from other interactions [5].

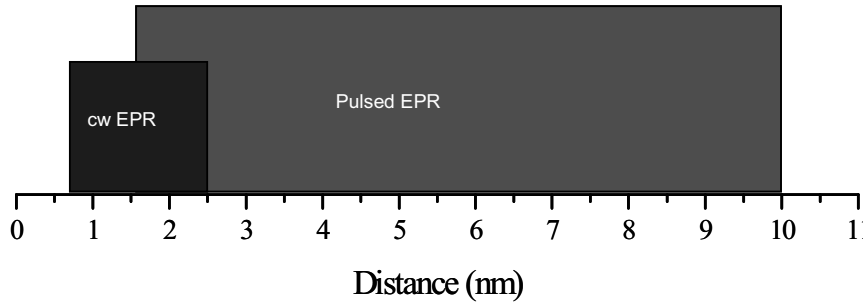

Fig. 6: Distance range covered by EPR spectroscopy. From 0.8 nm and 2.5 nm, the range covered by cw EPR. From 1.8 nm to 10 nm, the range covered by pulsed EPR.

1.4.1 Structure of a disordered system by cw EPR

The research described in Chapter 4 concerns the study of aggregation of peptides in membranes (lipid bilayers). Such systems are intrinsically disordered, and structural information can be obtained from cw EPR. If spin-labeled peptides aggregate in the membrane, the short distance between the spin labels (Fig. 7a) causes a broadening of the EPR spectra, which serves as an observable for aggregation. In Fig. 7c, the spectral effect of aggregation (broadening Δ) is shown. The broadening Δ is derived from the difference between a spectrum where the electron spins of the spin-labeled peptides interact (Fig. 7a) and the reference spectrum where the electron spins of the spin-labeled peptides are too far from each other to interact (Fig. 7b).
Whether aggregation occurs depends on the balance between peptide-peptide, lipid-peptide or lipid-lipid interactions. Therefore, it is interesting to study the aggregation of peptides at different conditions and phases of the lipids. Although broadening is an indication of aggregation, it is not sufficient in itself to prove aggregation and to describe the size and the geometry of the aggregate. The broadening for a pair of interacting electron spins is well established [6], but when spin-labeled peptides aggregate many the electron spins interact with each other and the broadening will be the result of their mutual interactions.

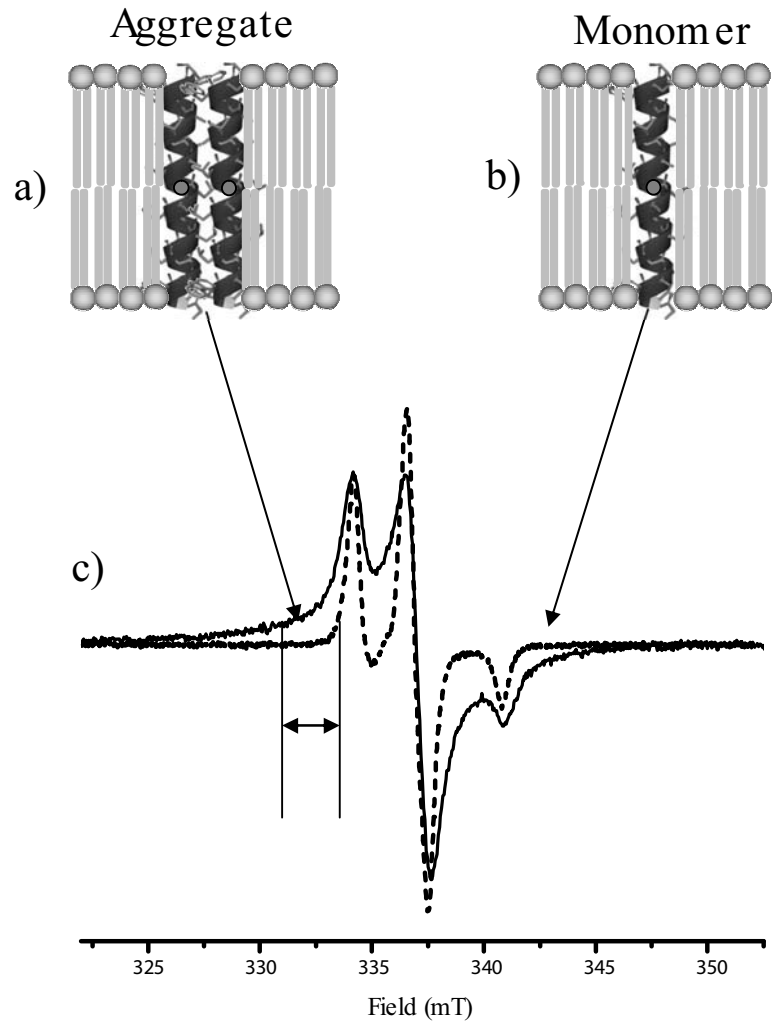

Fig. 7: Aggregation of peptides in membranes. (a) Side view of a peptide aggregate in a membrane. (b) Side view of a monomer of a peptide in a membrane. The gray circles in picture a) and b) indicate the position of the spin labels in the peptides. (c) The resulting EPR spectra of the aggregate (solid line) and of the monomeric spin-labeled peptides (dotted line). The Δ symbol indicates the broadening.

For a linear trimer aggregate (see Fig. 8b), for example, the spin label of the first peptide will interact not only with the spin label at a distance R (neighbour peptide), but it will interact also with the spin label at a distance of 2 R (third peptide). At the same time, the spin label of the second peptide will interact with the spin labels of both neighbouring peptides at a distance R. Therefore, a model that relates the broadening of the EPR spectra to the arrangement of the peptides in the lipids has been developed.

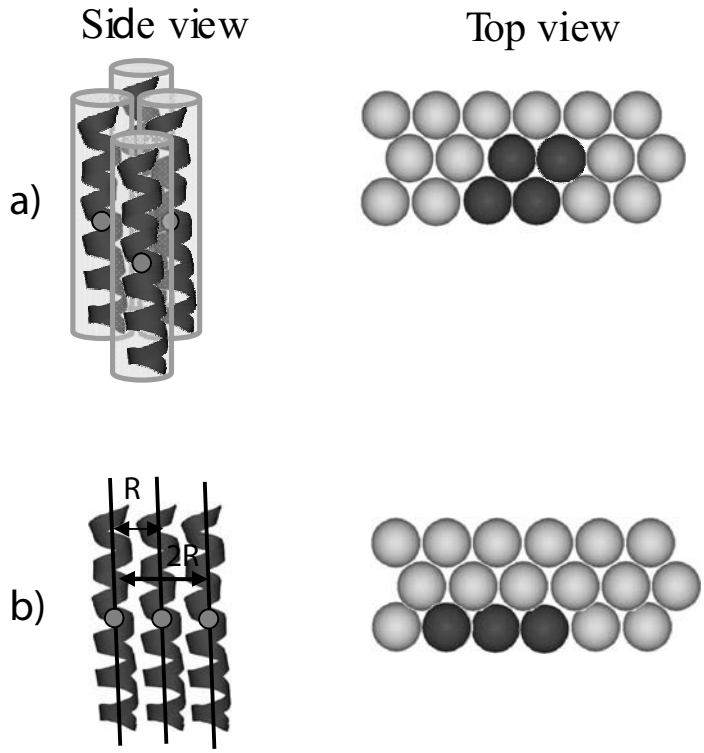

Fig. 8: Cluster and linear aggregates of peptides in membranes. (a) Side and top view of a cluster aggregate of spin-labeled peptides. (b) Side and top view of a linear aggregate of spin-labeled peptides. The gray circles in the side-view pictures indicate the position of the spin labels in the peptides. R indicates the distance between two neighbor peptides.

This model not only characterizes the dipolar broadening, but it relates the broadening to the size and the geometry of the aggregates. Comparing these under different lipid conditions reveals which of these conditions promotes the peptide-peptide interaction. In Fig. 8, examples of aggregates with different geometry and size are shown.

1.4.2 Distance measurement by pulsed EPR

Several pulsed EPR methods, such as the 2+1 sequence, the double electron-electron resonance (DEER) and the double-quantum coherence (DQC) [7-9], have been used in the last decade to measure distances and to determine the structure of chemical and biological systems by detecting the dipolar interaction between electron spins. These techniques are optimized for systems with low spectral anisotropy, such as nitroxide spin labels and organic radicals, and require that the pulses excite a large part of the spectrum. Transition-metal ions have a larger spectral width (anisotropy) than nitroxides and complete spectral excitation is not possible. In Fig. 9, the EPR spectra of a nitroxide and a transition-metal ion, an iron center, are superimposed. Whereas the nitroxide spectrum has a width of 10 mT, the spectrum of the metal center is 300 mT wide. The common pulsed methods have an excitation bandwidth of a few mT, e.g. a pulse length of 24 ns results in a bandwidth of 1.5 mT. For a system that involves a transition-metal ion, the resulting fractional excitation of the spectrum either severely limits the sensitivity or makes the application of these methods impossible. Therefore, to measure the distance between a nitroxide spin label and a transition-metal ion, different methods are needed. Such a method is the relaxation induced dipolar modulation (RIDME). Fig. 10b illustrates the three-pulse RIDME sequence. During the evolution time T, spontaneous flips of the spins of the transition-metal ion (B-spins), due to their longitudinal relaxation, occur. This causes modulation of the echo intensity of the spins of the nitroxide (A-spins), resulting in the dipolar trace (Fig. 10b). Therefore, there is no need to flip the B-spin by a pump pulse, avoiding the problem of the limited excitation bandwidth. Even though the three-pulse RIDME experiment is not affected by the limitation of the bandwidth, it suffers from a dead-time problem. For systems with large

spectral anisotropy, most of the information about the dipolar interaction lays in the initial part of the recorded dipolar-modulation time trace.

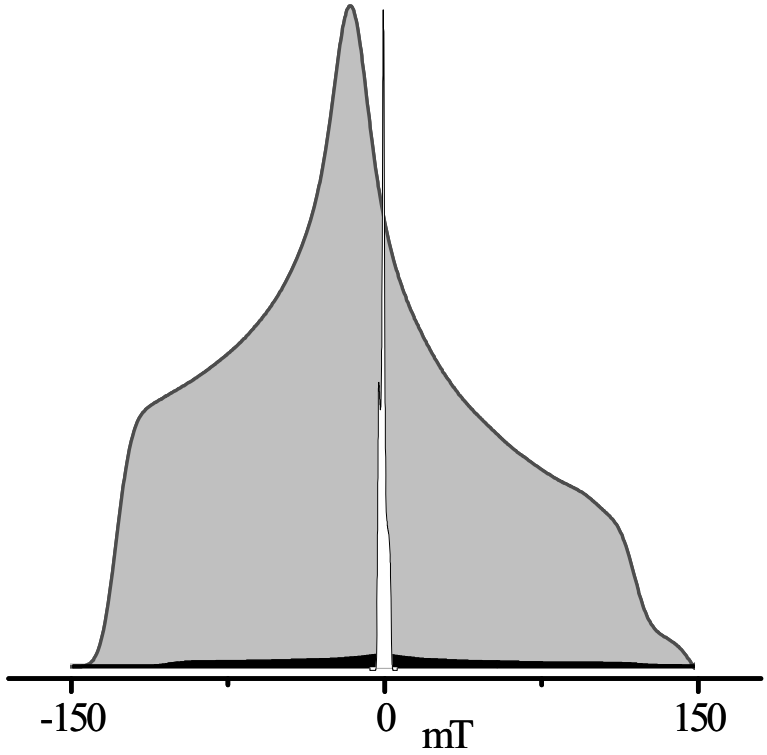

Fig. 9: The comparison between the EPR spectral width of a nitroxide spin-label and an iron(III) center (S=1/2). White-filled: the EPR spectrum (absorption mode) of the nitroxide. Black-filled: the EPR spectrum (absorption mode) of the iron center. Gray-filled: intensity of the black-filled spectrum multiplied by 30.

To detect the initial part of the trace, the inter-pulse separation τ has to be very short (see sequence in Fig. 10b). The problem is that τ can not be zero because the first and the second pulse should not overlap. Therefore, to avoid the dead-time problem, a new 5-pulse RIDME sequence has been developed.

In Chapter 5, this new sequence is introduced and its application to determine the distance between the low-spin iron(III) center and a nitroxide spin label (Fig. 10a) in spin-labeled cytochrome *f* is described.

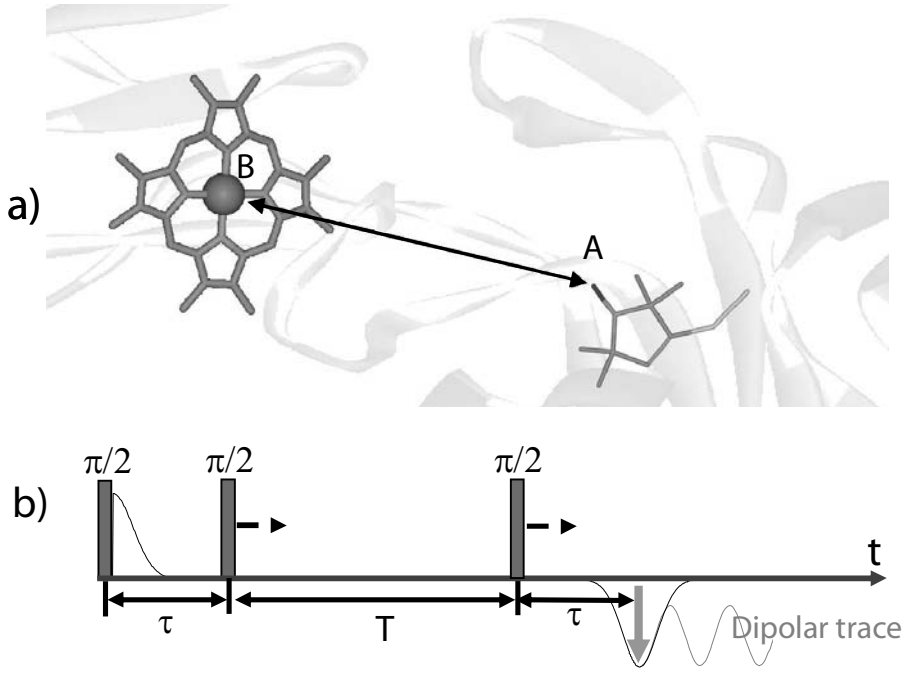

Fig. 10: (a) A schematic representation of iron center and of a nitroxide spin-label in a cytochrome *f* protein. The electron spins of the iron and of the nitroxide are indicated respectively by B and A. (b) The three-pulse RIDME sequence.

Reference list

1. Atherton, N. M. *Principles of Electron Spin Resonance;* Hellis Horwood Limited: Chichester, 1993.
2. Coremans, J. W. A.; Poluektov, O. G.; Groenen, E. J. J.; Canters, G. W.; Nar, H.; Messerschmidt, A. *Journal of the American Chemical Society* **1994,** *116* (7), 3097-3101.
3. Steinhoff, H. J.; Hubbell, W. L. *Biophysical Journal* **1996,** *71* (4), 2201-2212.
4. Berliner, L. J.; Eaton, S. S.; Eaton, G. R. *Biological Magnetic Resonance: Distance measurement in biological systems by EPR;* Kluwer Academic, New York: 2000.
5. Schweiger, A.; Jeschke, G. *Principles of Pulse Electron Paramagnetic Resonance;* Oxford University Press: 2001.
6. Steinhoff, H. J. *Frontiers in Bioscience* **2002,** *7*, C97-C110.
7. Kurshev, V. V.; Raitsimring, A. M.; Tsvetkov, Y. D. *Journal of Magnetic Resonance* **1989,** *81* (3), 441-454.
8. Milov, A. D.; Ponomarev, A. B.; Tsvetkov, Y. D. *Chemical Physics Letters* **1984,** *110* (1), 67-72.
9. Saxena, S.; Freed, J. H. *Chemical Physics Letters* **1996,** *251* (1-2), 102-110.